

Characterization of Spectral Regrowth in Microwave Amplifiers Based on the Nonlinear Transformation of a Complex Gaussian Process

Kevin G. Gard, *Member, IEEE*, Hector M. Gutierrez, *Member, IEEE*, and Michael B. Steer, *Fellow, IEEE*

Abstract—A statistical technique is presented for the characterization of spectral regrowth at the output of a nonlinear amplifier driven by a digitally modulated carrier in a digital radio system. The technique yields an analytical expression for the autocorrelation function of the output signal as a function of the statistics of the quadrature input signal transformed by a behavioral model of the amplifier. The amplifier model, a baseband equivalent representation, is derived from a complex radio-frequency envelope model, which itself is developed from readily available measured or simulated amplitude modulation–amplitude modulation and amplitude modulation–phase modulation data. The technique is used in evaluating the spectral regrowth for a CDMA signal.

Index Terms—Amplifier, CDMA, digital radio, nonlinear system.

I. INTRODUCTION

ONE OF THE important aspects of the cellular radio concept is the inherent tolerance to interference in the band of the communication channel. That is, in-band interference above that of background noise is expected, and system design accommodates this. In digital radio systems, the tolerable level of interference is determined by the ability of error-correction codes, added to the modulating bit stream, to correct for the bit errors that interference produces. The relatively lower acceptable interference levels in an analog radio is set for a subjectively determined minimum acceptable voice quality. In both analog and digital radio, in-band interference is largely due to signal transmission from other remote base stations or remote units using the same frequency channel, and by other radios using adjacent and alternate (the next, but one) channels. Thus, system interference budgeting requires transmitted intermodulation levels in the adjacent and alternate channels be limited so as not to cause interference to other radios operating in nearby channels. The type of modulation and baseband filtering determine the minimum level of adjacent channel

interference, even without nonlinear effects. The adjacent channel interference levels increase through the generation of out-of-band components by the nonlinear amplifier chain. This process of increasing adjacent channel interference with increasing transmitter power is called spectral regrowth or sideband regrowth.

Interference produced in the adjacent channel is characterized by the adjacent channel power ratio (ACPR), which is the power in the main channel divided by the power in the lower plus upper adjacent channels. Considering just the lower channel yields $ACPR_{\text{LOWER}}$ and the upper channel alone yields $ACPR_{\text{UPPER}}$. Analog cellular radio uses frequency or phase modulation, and ACPR is adequately characterized by intermodulation distortion of discrete tones. Typically, third-order intermodulation product (IP3) generation, in a two-tone test, is adequate to describe spectral regrowth. Thus, distortion in analog radio is accurately modeled using discrete tone steady-state simulation. Digital radio, however, uses complex modulation, and adjacent channel distortion has little relationship to intermodulation in a two-tone test [1], [2]. A modulated input signal applied to radio-frequency (RF) electronics in digital radio is a sophisticated waveform resulting from coding, filtering, and quadrature generation. It can neither be represented by a small number of discrete tones (or frequencies), nor can the waveform be represented in a simple analytic form. The only way the input stream can conveniently and accurately be represented is by its statistics, and transforming these using an appropriate behavioral model provides accurate and efficient modeling of ACPR and gain compression.

The purpose of this paper is to develop techniques for the prediction of ACPR and gain compression at the output of a nonlinear amplifier, represented as a behavioral model, from the statistics of the input modulated RF signal. The major contributions of this paper are as follows:

- 1) characterization of a digitally modulated signal by its autocorrelation functions, and using this with a behavioral nonlinear model to obtain the output statistics of the digitally modulated signal, from which the ACPR is obtained.
- 2) use of readily available amplitude modulation–amplitude modulation (AM–AM) and amplitude modulation–phase modulation (AM–PM) measurements (experimentally

Manuscript received September 1, 1998. This work was supported in part by the Defense Advanced Research Projects Agency under Agreement DAA-01-96-K-3619 as a MAFET III.

K. G. Gard is with Qualcomm Inc., San Diego, CA 92121 USA.

H. M. Gutierrez is with Mechanical Engineering Program, Division of Engineer Sciences, Florida Institute of Technology, Melbourne, FL 32901 USA.

M. B. Steer is with the Institute of Microwaves and Photonics, School of Electronic and Electrical Engineering, The University of Leeds, Leeds LS2 9JT, U.K.

Publisher Item Identifier S 0018-9480(99)05289-8.

obtained or derived from simulation) to derive a complex envelope behavioral model;

- 3) development of the relationship between an envelope behavioral model and the baseband equivalent behavioral model, which, for the first time, enables the envelope behavioral model to be transformed to an instantaneous nonlinear behavioral model, referred to here as the baseband equivalent instantaneous behavioral model;
- 4) prediction of the gain compression of a digitally modulated signal, which differs from that determined from AM-AM characterization largely because of nonunity peak-to-average effects.

II. BACKGROUND

The availability of accurate methods for the estimation of spectral regrowth is of particular interest to those involved in the design of cellular and personal communications systems where nonlinear devices, especially in the power amplifiers, generate co-channel and adjacent channel interference due to sideband regrowth. Stringent regulatory emission requirements directly affect the design of microwave power amplifiers. In particular, design choices that limit adjacent channel interference affect the efficiency and power output of RF active components by forcing them to operate in regimes that are closer to being linear. Thus, RF power amplifier design depends on tradeoffs of the following three main performance indicators:

- 1) output power;
- 2) efficiency;
- 3) sideband regrowth.

Hence, the importance of developing schemes to accurately predict ACPR and gain compression of an RF amplifier in a timely manner. ACPR is more difficult to predict than one- or two-tone responses since it depends not only on the intrinsic nonlinear behavior of the amplifier, but also on the encoding method and modulation format being used.

Estimation of spectral regrowth and intermodulation distortion has been approached in a variety of ways. Recently, Borges and Pedro [3] analyzed the excitation of a nonlinear circuit by a large number of input tones based on the spectral balance method and used the resulting algorithm to predict ACPR and noise-power ratio (NPR). A number of rapid system-level methods have been proposed to characterize spectral leakage to adjacent channels. Sevic *et al.* [4] used least squares fitting of a power series to AM-AM and AM-PM transfer data to predict amplitude and phase transformation through nonlinear microwave power transistors. It was found that ACPR can loosely correlate to the IP₃, although the presence of strong fifth-order nonlinearity, either due to loading or intrinsic device characteristics, can impact ACPR in the Japanese time-division multiple-access (TDMA) digital system. Leke and Kenney [5] generated analytical expressions for gain compression and phase distortion from a third-order Volterra nonlinear transfer function model and used these to predict spectral regrowth of a metal-semiconductor field-effect transistor (MESFET) power amplifier. Their method presents a connection between intermodulation distortion and

spectral regrowth, but is limited by the increasing complexity of the Volterra analysis for transfer functions above third order. While limited, Volterra nonlinear transfer function analysis provides valuable insight into the nonlinear process [2]. Chen *et al.* [6] developed a method to predict ACPR and NPR based on a time-domain analysis technique and bandpass nonlinearity theory. AM-AM and AM-PM transfer characteristics are used to directly predict samples of the output complex envelope based on samples of an input complex envelope and the algebraic expression for a bandpass nonlinearity given by the describing function and corresponding nonlinear phase and amplitude. AM-AM and AM-PM data is derived from measurements of complex gain versus input power for a one-tone signal. These are relatively straightforward and widely available to the RF designer. It can also be developed from discrete-tone steady-state (i.e., harmonic balance or shooting method) simulations. The method is limited to cases in which AM-AM and AM-PM characteristics provide a satisfactory representation of the device, leaving out biasing circuit memory effects and the effect of amplifier impedance mismatch. Lajoinie *et al.* [7] developed a modification of the method described by Chen *et al.* [6] that extends it to the prediction of NPR in amplifiers exhibiting nonlinear low-frequency dispersion (memory effects) such as satellite transponders. Sevic and Staudinger [8] presented a comparison of the behavioral model approach and a commercial envelope-simulation technique. The envelope-simulation technique does take into account nonlinear circuit memory effects, but has the disadvantages of requiring accurate circuit component models and prohibitive simulation run time.

While it is widely acknowledged that sideband regrowth depends on the encoding method (i.e., the statistics of the input stream), little work has been done to estimate output spectrum as the nonlinear transformation of an input random process. An early work in communication theory by Baum [9] revealed the general property of spectral regrowth when a Gaussian signal is passed through a nonlinear amplifier. Shimbo [10] developed a general formula for intermodulation for the case where arbitrary modulated carriers and Gaussian noise are amplified through a traveling-wave tube (TWT) system. Simplified expressions for certain types of nonlinearities, one of them power series, were also presented, although this paper does not discuss the nonlinear transformation of input signal moments. A landmark publication by Bedrosian and Rice [11] considered the case of nonlinear systems with memory and developed expressions for the Volterra transfer functions (Fourier transforms of the Volterra kernels) when the system equations are known and the system can be represented by a Volterra series. Output spectrum estimates are computed for two cases: when the input is zero-mean stationary Gaussian noise with known power spectrum and when the input is a sine wave plus zero-mean stationary Gaussian noise. Formulas for the output probability density function are also outlined, as they can be obtained by solving certain integral equations.

Recently, Wu *et al.* [12], [13] formulated a relationship between ACPR, IP₃, and fifth-order intermodulation product (IP₅) based on the output autocorrelation function of a real Gaussian random variable passed through an AM-AM non-

linear amplifier model. Their approach, however, is limited by several assumptions in the model and derivation. First, the authors use an AM–AM-only model asserting that AM–PM effects cannot be represented by a Taylor series expansion. However, a complex Taylor series expansion can account for both AM–AM and AM–PM effects of a memoryless non-linearity [14]–[16]. IP3 specifications are typically available for amplifiers, but IP5 and higher order terms are not. Thus, a designer must make IP5 measurements to obtain better accuracy in the ACPR estimate using the method described in [12]. Moreover, both AM–AM and AM–PM effects are easily extracted from single-tone complex gain measurements swept over input power [16]. Second, their derivation represents the CDMA waveform as a single real Gaussian random variable when the modulation signal is actually a complex sum of two random variables (the I and Q data channels). Third, the authors assume the power spectrum is flat over the modulation bandwidth when the actual signal spectrum shape is determined by a specific baseband filter response defined by the IS-95 CDMA standard [17]. Gutierrez *et al.* [18] have addressed most of these limitations by developing a closed-form expression for the autocorrelation of the amplifier output based on a moment theorem for complex Gaussian processes and an n th-order complex power-series model of the nonlinear amplifier. The output power spectrum is calculated from the Fourier transform of the output autocorrelation expression in terms of the input signal autocorrelation and, thus, does not make assumptions about the shape of the resulting output power spectrum. This allows convenient evaluation of the output spectrum for a variety of modulation formats by using estimates of the input autocorrelation function of each modulation format.

III. OUTPUT POWER SPECTRUM OF A COMPLEX GAUSSIAN SIGNAL PASSED THROUGH A NONLINEAR DEVICE

This section presents a method for predicting spectral regrowth based on the nonlinear transformation of the amplitude statistics of the input signal. A scheme that is simple to calculate and, therefore, more readily available to the practicing engineer seeking to estimate the nonlinear transfer response is developed. The proposed formulation seeks to provide design insight into how the nonlinearity affects the output spectrum by developing a modular approach that considers the successive transformation of the input statistics through the modulation scheme and the nonlinearity itself. The output power spectrum is estimated from an analytical expression for the output autocorrelation function that describes the transformation of a complex Gaussian signal when passed through a bandpass nonlinearity. The nonlinearity is modeled by a complex power series obtained from the measured or simulated AM–AM and AM–PM characteristics of the device.

The development proceeds with the two inputs to a quadrature modulator, treated as random signals with properties defined by their autocorrelation functions. The statistics at the output of the ideal quadrature modulator are derived and then applied to a nonlinear device characterized by a complex power-series-based nonlinear model. This leads to a statistical

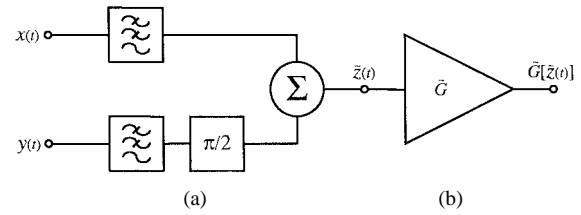


Fig. 1. (a) Quadrature modulator driving (b) a nonlinear device.

measure of a modulated signal at the output of a nonlinear device. Statistical analysis of digital communication systems utilizes a baseband equivalent representation, as shown in Fig. 1. There are subtle differences between the baseband equivalent behavioral model and corresponding RF envelope behavioral model, and this is discussed later in this section.

A. Input Signal Characterization

The digital quadrature-modulated signal $z(t)$ is statistically modeled as the complex addition of two independently filtered stationary random processes $x(t)$ and $y(t)$, each assumed to be zero mean

$$\tilde{z} = x(t) + jy(t) \quad (1)$$

where the tilde is used to indicate a quadrature signal. The variables here are voltage-like quantities; the power of each is proportional to the corresponding autocorrelation function, and each is assumed to be stationary. Thus, the notation is simplified by introducing subscripts to indicate quantities at different times as follows:

$$\begin{aligned} x_1 &= x(t) \\ x_2 &= x(t + \tau) \\ y_1 &= y(t) \\ y_2 &= y(t + \tau) \\ \tilde{z}_1 &= x_1 + jy_1 \\ \tilde{z}_2 &= x_2 + jy_2. \end{aligned} \quad (2)$$

Simplification is possible since the stationary assumption permits the time variable to be removed from the notation because the autocorrelation and cross-correlation sequences only depend on the time difference τ and not on absolute time. The autocorrelation function of a complex stationary random process $w(t)$ is defined as

$$\tilde{R}_{ww}(\tau) = E[\tilde{w}(t)\tilde{w}^*(t + \tau)] = E[\tilde{w}_1\tilde{w}_2^*] \quad (3)$$

where $E[\]$ is the expected value operator and $*$ denotes the complex conjugate. Since random processes $x(t)$ and $y(t)$ are stationary, the following correlation identities apply [19]:

$$\begin{aligned} R_{xx}(\tau) &= R_{yy}(\tau) = E[x_1x_2] = E[y_1y_2] \\ R_{xx}(0) &= E[x_1x_1] = E[x_2x_2] = E[y_1y_1] = E[y_2y_2] \\ R_{xy}(\tau) &= -R_{yx}(\tau) = E[x_1y_2] = -E[x_2y_1]. \end{aligned} \quad (4)$$

The autocorrelation of the quadrature process $z(t)$ can now be written as

$$\begin{aligned}\tilde{R}_{zz}(\tau) &= E\left[\tilde{z}(t)\tilde{z}^*(t+\tau)\right] \\ &= E[\tilde{z}_1\tilde{z}_2^*] \\ &= E\left[(x_1 + jy_1)(x_2 - jy_2)\right] \\ &= E\left[x_1x_2 + y_1y_2 + j(x_2y_1 - x_1y_2)\right] \\ &= 2R_{xx}(\tau) - j2R_{xy}(\tau).\end{aligned}\quad (5)$$

$R_{zz}(\tau)$ defines the statistics of the modulator's output, which is the signal input to the nonlinear device. It should be noted that the real part of the autocorrelation function is an even function and the imaginary part is an odd function about $\tau = 0$. The average power P_{zz} of the input signal $z(t)$ is proportional to the autocorrelation function evaluated at $\tau = 0$

$$\begin{aligned}P_{zz} &= A\tilde{R}_{zz}(0) \\ &= A\left\{2R_{xx}(0) - jR_{xy}(0)\right\} \\ &= 2AR_{xx}(0).\end{aligned}\quad (6)$$

Here, A is a power scaling variable used to set the input power level.

The nonlinear device can be characterized in part using single-tone measurements and can be represented as a band-pass nonlinearity with complex transfer characteristic [6], [16]

$$\tilde{G}(z) = \sum_{i=1}^N \tilde{a}_i \tilde{z} + \tilde{a}_3 \tilde{z}^3 + \tilde{a}_5 \tilde{z}^5 + \dots + \tilde{a}_N \tilde{z}^N \quad (7)$$

where \tilde{a}_i is a complex power-series coefficient. Only the odd terms can be determined from single-tone complex compression characteristics, but fortunately, the odd-order terms are the most important as they produce intermodulation distortion in-band and adjacent to the desired signal. Characterization of the nonlinear device is not the subject of this paper, as the use of complex power series to represent device nonlinearity at the circuit level has been extensively discussed in the literature [15]. It is important to realize that (7) represents a general nonlinear transfer characteristic and is not a gain expression. A general expression for nonlinear gain in a power-series nonlinearity is developed in the Appendix from this general nonlinear transfer characteristic. For the purpose of this paper, carrier effects will not be considered and, therefore, (7) is a valid starting point. This can be further illustrated by showing that a gain expression can also be obtained from (7) by using generalized power-series analysis, as will be illustrated in the following section. This provides the necessary translation to convert the envelope behavioral model to the baseband equivalent behavioral model.

B. Nonlinear Gain in a Power-Series Nonlinearity

Consider a nonlinear system described by a complex power series with an N -component multifrequency input $x(t)$

$$x(t) = \sum_{k=1}^N |X_k| \cos(\omega_k t + \phi_k)$$

where X_k is the phasor of the k th input tone. A phasor component of the output Y_q with radian frequency ω_q can be expressed as a sum of intermodulation products U , as described in [20], [21]

$$Y_q = \sum_{n=0}^{\infty} \sum_{\substack{n_1, \dots, n_N \\ |n_1| + \dots + |n_N| = n}} U(n_1, \dots, n_N)$$

where a set of n_k 's define an intermodulation product and n is the intermodulation order. In order to analyze such a problem numerically, the number of output frequency components can be truncated to N . The output of the power series driven by such input can then be computed by multinomial expansion and terms collected according to frequency, yielding an intermodulation product as

$$\begin{aligned}U_q(n_1, \dots, n_N) &= K(n_1, \dots, n_N) \left[1 + T'(n_1, \dots, n_N)\right] \\ K(n_1, \dots, n_N) &= \varepsilon_n \tilde{a}_n \frac{n!}{2^N} \operatorname{Re} \left\{ \prod_{k=1}^N \frac{(X_k^+)^{|n_k|}}{|n_k|!} \right\}_{\omega_q} \\ T'(n_1, \dots, n_N) &= \sum_{\alpha=1}^{\infty} \sum_{\substack{S_1, \dots, S_N \\ S_1 + \dots + S_N = \alpha}} \left(\frac{(n+2\alpha)!}{n! 2^{2\alpha}} \right) \\ &\quad \cdot \frac{\tilde{a}_{n+2\alpha}}{\tilde{a}_n} \prod_{k=1}^N \frac{|X_k|^{2S_k} |n_k|!}{S_k! (|n_k| + S_k)!}.\end{aligned}$$

The S_k are integer sequences defined by the summation index α ; the Neuman factor ε_n is one for $n = 0$ and two otherwise, and X_k^+ is equal to X_k for $n_k > 0$, and equal to its complex conjugate otherwise. Considering only first-order intermodulation, ($n = 1$) enables gain compression to be described. Restricting the analysis to first-order intermodulation ensures that the component of the output signal extracted is that part correlated with the input signal and not in-band distortion components. The output is also a single tone, which can be obtained from the expression above. For this component, the intermodulation term is

$$K_1 = 2\tilde{a}_1 \frac{1!}{2} X_1 = \tilde{a}_1 X_1$$

and the corresponding saturation term is

$$T' = \sum_{\alpha=1}^{\alpha_m} \frac{(1+2\alpha)!}{2^{2\alpha}} \frac{\tilde{a}_{1+2\alpha}}{\tilde{a}_1} \frac{|X_1|^{2\alpha}}{\alpha!(1+\alpha)!}.$$

This yields the phasor of the output

$$Y_1 = \tilde{a}_1 X_1 + \sum_{\alpha=1}^{\alpha_m} \tilde{a}_{1+2\alpha} \frac{(1+2\alpha)!}{2^{2\alpha} \alpha! (1+\alpha)!} |X_1|^{2\alpha} X_1. \quad (8)$$

The terms on the right-hand side that depend on α can be lumped with the coefficients of the behavioral model yielding

$$Y_1 = \tilde{a}_1 X_1 + \sum_{\alpha=1}^{\alpha_m} b_{1+2\alpha} |X_1|^{2\alpha} X_1. \quad (9)$$

This corresponds to the standard nonlinear gain expression. This expression relates a phasor at the input to the phasor at the output and corresponds to the complex gain measured in

the AM–AM and AM–PM characterization. However, evaluation of the power series requires a baseband equivalent behavioral model, which is an instantaneous power series. The relationship between the envelope behavioral model (9) and the baseband equivalent behavioral model [a complex power series for instantaneous quantities, such as (7)] is obtained by comparing (8) and (9). Thus, the $(1 + 2\alpha)$ coefficient of the baseband equivalent behavioral model is

$$\tilde{a}_{1+2\alpha} = b_{1+2\alpha} \frac{2^{2\alpha} \alpha! (1 + \alpha)!}{(1 + 2\alpha)!}, \quad \alpha = 1, \dots, \alpha_m. \quad (10)$$

The procedure for developing the baseband equivalent behavioral model, as required in predicting spectral regrowth, is as follows. First, fitting a complex polynomial to AM–AM and AM–PM measurements leads to a complex power series (9) with coefficients b_i [1], [2], [15]. This is not an instantaneous power series, but relates the complex envelope of the input signal (a phasor of a single-tone signal) to the complex envelope of the output signal (again, a phasor for a single-tone signal). The signal transformation presented here requires an instantaneous nonlinear model, not its phasor form. As the carrier is not included in the envelope behavioral model, the instantaneous form is the baseband equivalent behavioral model (7) with coefficients a_i obtained by applying (10).

C. Output Power Spectrum of a Quadrature Signal Passed Through a Power-Series Nonlinearity

The power spectrum of the signal at the output of the nonlinear device is found from the autocorrelation function of the output signal $R_{gg}(\tau)$ calculated by applying (4) to the baseband equivalent polynomial model (7) with coefficients \tilde{a}_i

$$\begin{aligned} \tilde{R}_{gg}(\tau) &= E \left[\tilde{G}(\tilde{z}_1) \tilde{G}^*(\tilde{z}_2) \right] \\ &= E \left[\left\{ \tilde{a}_1 \tilde{z}_1 + \tilde{a}_2 \tilde{z}_1^3 + \tilde{a}_3 \tilde{z}_1^5 + \tilde{a}_5 \tilde{z}_1^7 \right\} \right. \\ &\quad \left. \cdot \left\{ \tilde{a}_1^* \tilde{z}_2^* + \tilde{a}_3^* (\tilde{z}_2^*)^3 + \tilde{a}_5^* (\tilde{z}_2^*)^5 \right\} \right] \\ &= |\tilde{a}_1|^2 E[\tilde{z}_1 \tilde{z}_2^*] + \tilde{a}_1 \tilde{a}_3^* E[\tilde{z}_1 (\tilde{z}_2^*)^3] + \tilde{a}_1 \tilde{a}_5^* E[\tilde{z}_1 (\tilde{z}_2^*)^5] \\ &\quad + \tilde{a}_1^* \tilde{a}_3 E[\tilde{z}_1^3 \tilde{z}_2^*] + |\tilde{a}_3|^2 E[\tilde{z}_1^3 (\tilde{z}_2^*)^3] + \tilde{a}_3 \tilde{a}_5^* E[\tilde{z}_1^3 (\tilde{z}_2^*)^5] \\ &\quad + \tilde{a}_1^* \tilde{a}_5 E[\tilde{z}_1^5 \tilde{z}_2^*] + \tilde{a}_3 \tilde{a}_5^* E[\tilde{z}_1^5 (\tilde{z}_2^*)^3] \\ &\quad + |\tilde{a}_5|^2 E[\tilde{z}_1^5 (\tilde{z}_2^*)^5] + \dots \end{aligned} \quad (11)$$

Expanding $R_{gg}(\tau)$ results in many algebraically intensive moment manipulations involving $x(t)$ and $y(t)$, i.e., $\tilde{z}(t) = x(t) + jy(t)$. Fortunately, a previous result for the moments of complex Gaussian random variables [22] can be used to calculate each of the terms in this expression, namely,

$$\begin{aligned} &E \left[\tilde{z}_1 \tilde{z}_2, \dots, \tilde{z}_s \tilde{z}_1^* \tilde{z}_2^*, \dots, \tilde{z}_t^* \right] \\ &= \begin{cases} 0, & s \neq t \\ \sum_{\pi} E \left[\tilde{z}_{\pi(1)} \tilde{z}_1^* \right] E \left[\tilde{z}_{\pi(2)} \tilde{z}_2^* \right], \dots, E \left[\tilde{z}_{\pi(s)} \tilde{z}_t^* \right], & s = t. \end{cases} \end{aligned} \quad (12)$$

Here, π is a permutation of the set of integers $\{1, 2, \dots, s, \dots, t\}$, and $\{\tilde{z}_i, i = 1, 2, \dots, s, \dots, t\}$ denotes a set of complex independent Gaussian random variables. Application of (12) yields the following identity:

$$E[\tilde{z}_1 \tilde{z}_2 \tilde{z}_3^* \tilde{z}_4^*] = E[\tilde{z}_1 \tilde{z}_3^*] E[\tilde{z}_2 \tilde{z}_4^*] + E[\tilde{z}_2 \tilde{z}_3^*] E[\tilde{z}_1 \tilde{z}_4^*]$$

and, most importantly,

$$E \left[(\tilde{z}_1 \tilde{z}_2^*)^n \right] = n! E[\tilde{z}_1 \tilde{z}_2^*]^n = n! \tilde{R}_{zz}^n(\tau). \quad (13)$$

Assuming that the input random processes are Gaussian allows the expanded form of the output autocorrelation function (11) to be simplified, yielding the following compact expression:

$$\begin{aligned} \tilde{R}_{gg}(\tau) &= |\tilde{a}_1|^2 A \tilde{R}_{zz}(\tau) + 3! |\tilde{a}_3|^2 A^3 \tilde{R}_{zz}^3(\tau) \\ &\quad + \dots + N! |\tilde{a}_N|^2 A^N \tilde{R}_{zz}^N(\tau) \\ &= \sum_{\substack{n=1 \\ n \text{ odd}}}^N n! |\tilde{a}_n|^2 A^n \tilde{R}_{zz}^n(\tau) \end{aligned} \quad (14)$$

where, again, A is a power scaling variable used to set the input power level. Evaluation of the output power spectrum requires an estimate of the input autocorrelation function $R_{zz}(\tau)$ of the complex input process $z(t)$. A closed-form analytical expression for this is usually difficult to derive; however, good estimates can be obtained by using long independent data sequences passed through a quadrature modulator. Input autocorrelation is then estimated by applying a sliding discrete correlator to the sum of the two Gaussian input streams $x(t)$ and $y(t)$, after passing them through a hard limiter (sign function) and an finite-impulse response (FIR) baseband filter. This generates an input stream as defined by the CDMA IS-95 standard [17]. The output autocorrelation function, (14), is then defined by powers of the input autocorrelation function, an input scaling factor, and the magnitudes of the power-series coefficients. It is interesting to note that all of the cross terms in the expansion of $R_{gg}(\tau)$ are zero as a result of the moment theorem [22]. The output power spectrum $\tilde{S}_{gg}(f)$ is obtained as the Fourier transform of the output autocorrelation (14)

$$\begin{aligned} \tilde{S}_{gg}(f) &= \int_{-\infty}^{\infty} \tilde{R}_{gg}(\tau) e^{j2\pi f\tau} d\tau \\ &= \sum_{n=1}^N n! |\tilde{a}_n|^2 A^n \int_{-\infty}^{\infty} \tilde{R}_{zz}^n(\tau) e^{-2\pi f\tau} d\tau \\ &= \sum_{\substack{n=1 \\ n \text{ odd}}}^N n! |\tilde{a}_n|^2 A^n F \left\{ \tilde{R}_{zz}^n(\tau) \right\} \end{aligned} \quad (15)$$

where

$$F \left\{ \tilde{R}_{zz}^n(\tau) \right\} = \int_{-\infty}^{\infty} \tilde{R}_{zz}^n(\tau) e^{-j2\pi f\tau} d\tau.$$

Thus, the output power spectrum is the sum of the individual spectra of each term in the power series, scaled by its corresponding coefficient and input power level. When computing the output spectrum, the Fourier transform of each spectral component is calculated first, then scaled by the input

power level and the corresponding power-series coefficient, and added as in (15) to yield $\tilde{S}_{gg}(f)$. This derivation shows that only the input autocorrelation function $R_{zz}(\tau)$ and complex power-series description are necessary to estimate the output power spectrum of the nonlinear device.

IV. POWER RELATIONSHIPS

The output power spectrum must, in general, be evaluated numerically, but the total output power can be evaluated much more simply. From (6), total output power can be calculated by setting $\tau = 0$ in the output autocorrelation function (14). The output power can, therefore, be expressed as the sum of linear signal power and intermodulation power components

$$\begin{aligned}
 P_{gg} &= \tilde{R}_{gg}(0) \\
 &= \sum_{n=1}^N n! |\tilde{a}_n|^2 \tilde{R}_{zz}^n(0) \\
 &= \sum_{\substack{n=1 \\ n \text{ odd}}}^N n! |\tilde{a}_n|^2 A^n 2^n R_{xx}^n(0) \\
 &= \sum_{\substack{n=1 \\ n \text{ odd}}}^N n! |\tilde{a}_n|^2 P_{in}^n.
 \end{aligned} \tag{16}$$

Thus, both output power and intermodulation power only depend on the nonlinear transfer characteristics and input signal power. Total power is independent of the shape of the power spectrum and the intermodulation power spectrum. However, ACPR measurements are typically defined as a ratio of main to adjacent channel spectral power, which is dependent on the particular shape of the modulation power spectrum. The spectral shape of each intermodulation component does not change as a function of input power, only the total power of that component is affected. As a result, the amount of power at a specific frequency band of the intermodulation spectrum is a fixed fraction of the total power of that component

$$P_{gg}(n) = n! |\tilde{a}_n|^2 F_n P_{in}^n$$

where F_n is the fractional intermodulation power coefficient. Each F_n coefficient is calculated as a ratio of intermodulation power (at the specified offset and bandwidth) to total distortion power for the corresponding nonlinear spectral component.

In addition to out-of-band intermodulation power, each wireless standard specifies a baseband data filter, which sets a lower limit on ACPR due to the finite rejection of the filter. Filtering effects can be accommodated by adding an extra out-of-band component to the intermodulation power to represent the finite filter rejection

$$P_{\text{filter}} = 10^{-\alpha/10} |\tilde{a}_1|^2 P_{in}$$

where α is the filter adjacent channel rejection in decibels.

V. ACPR

Adjacent channel power arises from spectrum regeneration, the process by which a band-limited digitally modulated signal

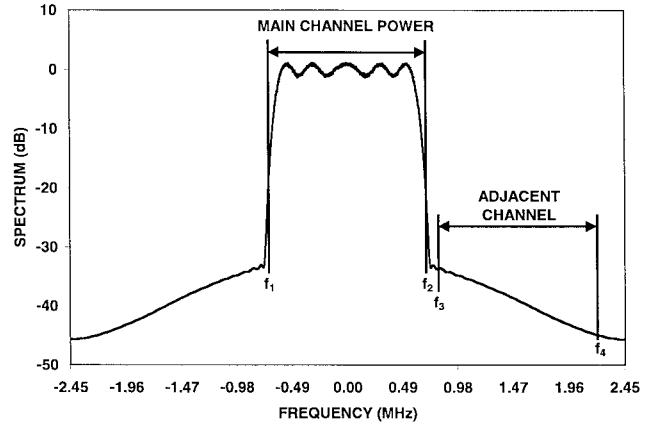


Fig. 2. Definition of ACPR.

is applied to a nonlinearity, thus causing a portion of the band-limited spectrum to leak into adjacent frequency bands due to intermodulation. ACPR is defined differently in the various wireless standards, the main difference being the way in which adjacent channel power affects the performance of another wireless receiver for which the offending signal is co-channel interference. In general, upper channel ACPR is defined as

$$\text{ACPR}_{\text{UPPER}} = \frac{\int_{f_3}^{f_4} \tilde{S}_{gg}(f) df}{\int_{f_1}^{f_2} \tilde{S}_{gg}(f) df} \tag{17}$$

where frequencies f_1 and f_2 are the frequency limits of the main channel, and f_3 and f_4 are the limits of the lower adjacent channel. The denominator clearly represents the power in the main channel. This definition is illustrated in Fig. 2.

In the IS-95 Standard [17], ACPR is defined as the ratio of the adjacent channel power in a 30-kHz resolution bandwidth (i.e., $f_4 - f_3 = 30$ kHz), swept over the adjacent channel, to the total power in the main channel ($f_2 - f_1 = 1.23$ MHz). The ACPR results presented here are measured at an 885-kHz offset from the channel center frequency since maximum ACPR typically occurs at the closest band edges to the main channel. Also, the main channel power is normalized to a 30-kHz bandwidth to allow the ACPR measurement to relate directly to decibels referred to carrier power (dBc) difference between the main and adjacent channel power when using a spectrum analyzer to measure ACPR.

An output power spectrum estimate, such as the one given by (15), can easily be used to estimate ACPR. This is done by calculating the integrals in (17) based on adding the magnitudes of the components of the discrete spectrum over the corresponding frequency bands. Notice that (15) is calculated from a fast Fourier transform (FFT) of the output autocorrelation and, therefore, provides a discrete estimate of the spectrum.

From the discussion in the previous section, the effect of filtering can be incorporated into an ACPR measurement by computing the F_n intermodulation power coefficients corresponding to the specified adjacent channel definition and then taking the ratio of the main channel to the total adjacent

TABLE I
COEFFICIENTS OF THE COMPLEX POWER-SERIES
MODEL OF THE NONLINEAR DEVICE

Order	Polynomial coefficient
1	14.74374 + j2.134037
3	-67.08899 - j20.62420
5	-6345.0940 + j2646.8041
7	-202512.98 - j50291.11
9	1.7298x10 ⁷ - j1.0464x10 ⁶
11	-3.2843x10 ⁸ + j3.767x10 ⁷
13	1.9960x10 ⁹ - j2.788x10 ⁸

channel intermodulation power

$$\begin{aligned}
 \text{ACPR} &= \frac{P_{gg}(1)}{P_{\text{filter}} + \sum_{n=3}^N P_{gg}(n)} \\
 &= \frac{|\tilde{a}_1|^2 P_{\text{in}}}{10^{-\alpha/10} |\tilde{a}_1|^2 P_{\text{in}} + \sum_{n=3}^N n! |\tilde{a}_n|^2 F_n P_{\text{in}}^n} \\
 &= \frac{1}{10^{-\alpha/10} + \sum_{n=3}^N n! \left| \frac{\tilde{a}_n}{\tilde{a}_1} \right|^2 F_n P_{\text{in}}^{n-1}}.
 \end{aligned}$$

Thus, determination of ACPR requires separate estimation through numerical integration of the output spectral density in the main and adjacent channels.

VI. EXPERIMENTAL RESULTS

A. Behavioral Model

The AM–AM and AM–PM curves for a 900-MHz CDMA power amplifier with 23-dB gain were obtained using a single-frequency input power sweep and a vector network analyzer [23]. A complex power series of order 13 was fitted to the AM–AM and AM–PM data from a 900-MHz CDMA power amplifier using least-squares optimization. The resulting envelope behavioral model coefficients are shown in Table I. These were transformed into the baseband equivalent instantaneous behavioral model using (10).

The complex power-series model was verified by comparing measured and predicted AM–AM and AM–PM data. The quality of the fit is illustrated in Fig. 3, where measured AM–AM and AM–PM data are plotted by the solid line and interpolated values obtained from the envelope power-series model are shown by the dashed lines.

B. ACPR Estimation Based on the Nonlinear Transformation of the Autocorrelation Function

Evaluation of the output power spectrum requires an estimate of the input autocorrelation function $R_{zz}(\tau)$ of the complex input process $z(t)$. Input autocorrelation was estimated using a biased autocorrelation estimator [24] applied to 2¹⁹-b-long Gaussian input streams $x(t)$ and $y(t)$ after passing

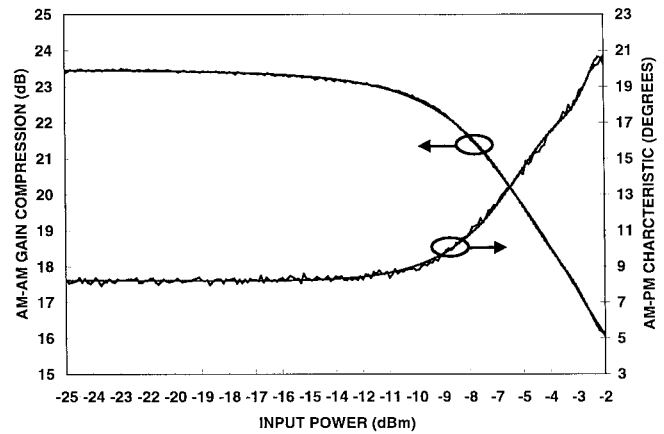


Fig. 3. Measured and predicted AM–AM and AM–PM data.

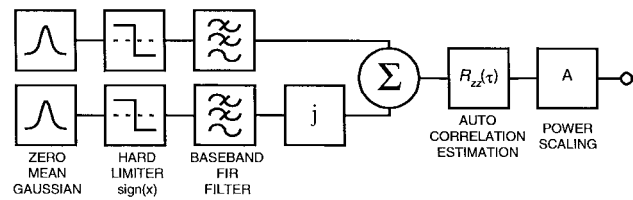


Fig. 4. Estimation of input autocorrelation.

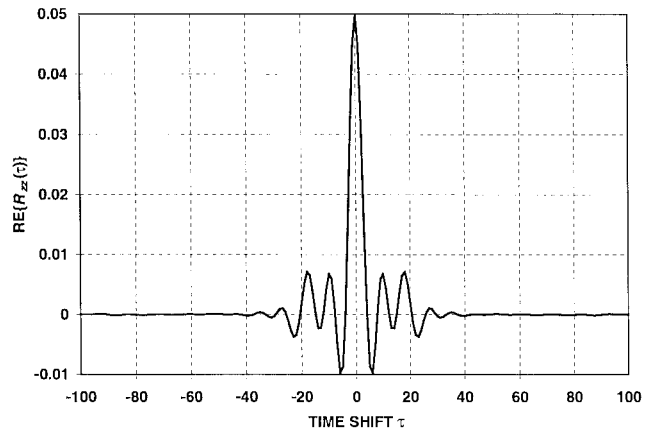


Fig. 5. Estimate of input autocorrelation function.

them through a hard limiter (sign function) and a FIR baseband filter, as shown in Fig. 4. An input stream generated this way mimics the statistical properties of a communication channel as defined by the CDMA IS-95 Standard [17]. The estimated CDMA autocorrelation function is shown in Fig. 5.

The input autocorrelation and baseband equivalent behavioral model (7) were used in (15) to estimate output power spectrum. Estimated spectra for several output power levels are shown in Fig. 6.

The calculations outlined in Sections II and III use a complex envelope baseband representation of the signal, which introduces a factor of two in the power spectral density of uncorrelated terms [25]. For this reason, the spectral components corresponding to nonlinear distortion [terms in (15) with $n > 1$] have been weighted by a factor of 0.5. ACPR was

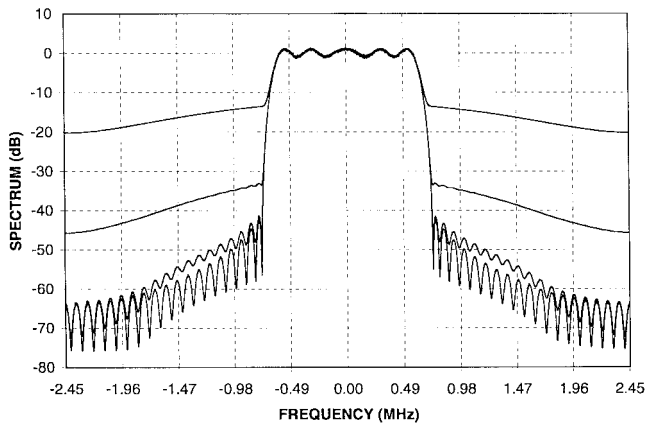


Fig. 6. Spectrum estimates based on the transformation of input autocorrelation. Increasingly higher curves for 0-, 5-, 10-, and 13-dBm output power are shown.

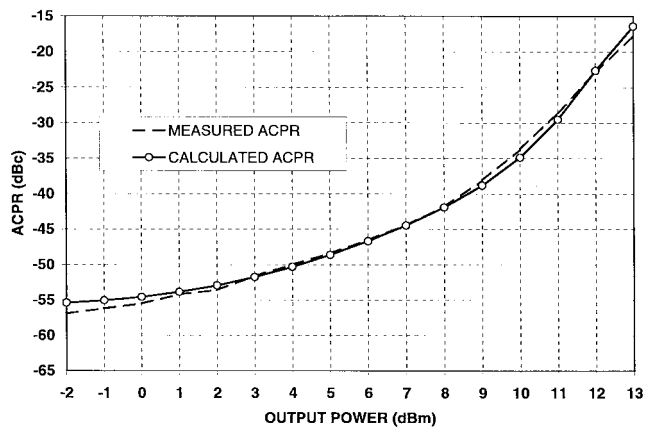


Fig. 7. Measured versus predicted ACPR from estimation of spectral regrowth.

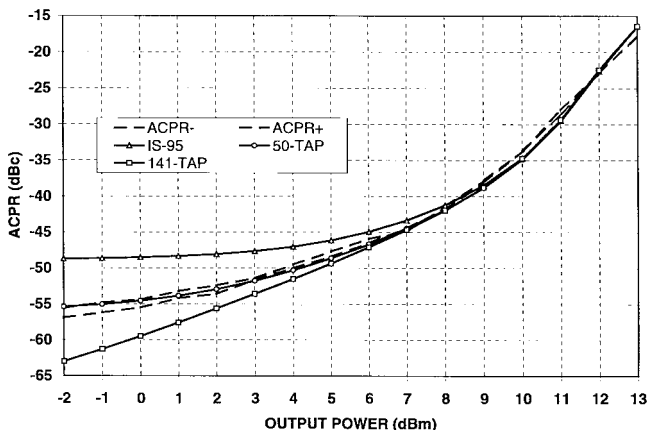


Fig. 8. Effect of input filtering on ACPR estimation.

then calculated as described in [1] and compared with ACPR measurements. Results are shown in Figs. 7 and 8.

The number of taps of the FIR filter (see Fig. 4) affects the method's performance at low output power levels due to the difference in stopband characteristics. It is possible to find a filter size that yields an optimal fit between measured and predicted ACPR, as can be seen in Fig. 8.

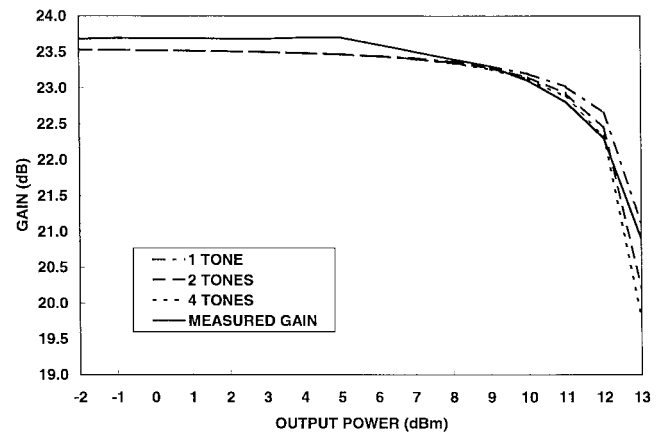


Fig. 9. Prediction of nonlinear compression characteristics based on generalized power-series analysis.

C. Gain Compression

The generalized power-series analysis can be used to predict gain compression in the nonlinear device by simulating the saturation term (T') at different input power levels. Results are shown in Fig. 9, where the solid line represents measured CDMA gain as a function of output power level, and the dashed and dotted lines correspond to compression factor (T'), calculated for different multifrequency inputs whose power match the measured available power, and scaled by the linear gain coefficient a_1 . The one-tone result corresponds to the measured AM-AM characteristic. The multitone analysis models the gain compression of the digital signal. The amplitudes of the phasors in (7) were derived from the input signal power considering that tones were uncorrelated.

The AM-AM gain curve is coincident with the one-tone since it was measured using a single tone.

VII. CONCLUSIONS

A method for the estimation of spectral regrowth on digitally modulated signals passed through a nonlinear device modeled by a complex power series has been presented. The proposed method considers the nonlinear transformation of the input autocorrelation function and takes advantage of statistical properties of moments of a complex Gaussian random variable to develop a simple expression for the autocorrelation of the output signal; hence, providing an output spectrum estimate from which ACPR can easily be calculated. This method has the advantage of providing mathematical insight into the transformation of the input statistics.

There are limitations to the procedure presented here. Single-tone AM-AM and AM-PM models cannot take into account baseband effects due to the nature of the test from which the coefficients are extracted [18]. Even when the AM-PM measurements are obtained from a complex modulation envelope, spectral regrowth in amplifiers presenting hysteresis cannot be predicted by a complex power-series model within a 1-dB error unless a model with memory is used [7]. As analytic formulations of the input statistics are not available, a discrete estimator of the autocorrelation function of the input signal is necessary. The behavioral

model is derived from single-tone envelope characterizations and, therefore, describes only odd-order intermodulation. The actual statistical distribution of the input streams depends on the modulation format and, thus, spectral regrowth will also be dependent on modulation format and possibly encoding schemes.

APPENDIX

This section derives a general gain expression for a modulated carrier passing through a memoryless bandpass nonlinearity considering carrier effects. The development here is an extension of earlier related work [14, Sec. 2.11.7.2]. Consider an AM and PM carrier $w(t)$ with carrier frequency ω_c

$$\begin{aligned} w(t) &= A(t) \cos[\omega_c t + \theta(t)] \\ &= \frac{A(t)}{2} \left[e^{j\omega_c t} e^{j\theta(t)} + e^{-j\omega_c t} e^{-j\theta(t)} \right] \\ &= \frac{1}{2} \left[\tilde{z}(t) e^{j\omega_c t} + \tilde{z}^*(t) e^{-j\omega_c t} \right] \end{aligned} \quad (\text{A.1})$$

where $A(t)$ and $\theta(t)$ are the AM and PM, and $z(t)$ the quadrature signal

$$\tilde{z}(t) = A(t) e^{j\theta(t)} = x(t) + jy(t). \quad (\text{A.2})$$

Using the binomial expansion to compute the n th power of $w(t)$ yields

$$\begin{aligned} w^n(t) &= \left\{ \frac{1}{2} \left[\tilde{z}(t) e^{j\omega_c t} + \tilde{z}^*(t) e^{-j\omega_c t} \right] \right\}^n \\ &= \frac{1}{2^n} \sum_{k=0}^n \binom{n}{k} \left[\tilde{z}(t) \right]^k \left[\tilde{z}^*(t) \right]^{n-k} e^{j\omega_c(2k-n)t}. \end{aligned} \quad (\text{A.3})$$

Consider now only the frequency terms centered at the carrier frequency (this is usually referred to as the first zonal filter at the output of the nonlinearity). This implies $2k - n = \pm 1$ for odd n only. Equation (A.3) then becomes

$$w^n(t) = \frac{1}{2^{n-1}} \binom{n}{\frac{n+1}{2}} \left[\tilde{z}(t) \tilde{z}^*(t) \right]^{(n-1)/2} \tilde{z}(t). \quad (\text{A.4})$$

Combining (A.4) with the complex gain expression (7) yields the bandpass nonlinear gain expression

$$\tilde{G}(z) = \tilde{z}(t) \sum_{n=1}^N \frac{\tilde{a}_n}{2^{n-1}} \binom{n}{\frac{n+1}{2}} \left[\tilde{z}(t) \tilde{z}^*(t) \right]^{(n-1)/2}. \quad (\text{A.5})$$

For instance, for $N = 13$, and the modulation being just the carrier (i.e., $z(t) = A$, where A is the carrier voltage amplitude)

$$\begin{aligned} \tilde{G}(z) &= \sum_{n=1}^N \frac{\tilde{a}_n}{2^{n-1}} \binom{n}{\frac{n+1}{2}} A^n \\ &= \tilde{a}_1 A + \tilde{a}_3 \frac{3}{4} A^3 + \tilde{a}_5 \frac{5}{8} A^5 + \tilde{a}_7 \frac{35}{64} A^7 + \tilde{a}_9 \frac{63}{128} A^9 \\ &\quad + \tilde{a}_{11} \frac{231}{512} A^{11} + \tilde{a}_{13} \frac{429}{1024} A^{13} \end{aligned} \quad (\text{A.6})$$

In general, the output autocorrelation is obtained by taking the moments of (A.5)

$$\begin{aligned} \tilde{R}_{gg}(\tau) &= E \left[\tilde{G}(\tilde{z}_1) \tilde{G}^*(\tilde{z}_2) \right] \\ &= E \left\{ \left[\tilde{z}_1 \sum_{n=1}^N \frac{\tilde{a}_n}{2^{n-1}} \binom{n}{\frac{n+1}{2}} [\tilde{z}_1 \tilde{z}_1^*]^{(n-1)/2} \right] \right. \\ &\quad \cdot \left. \left[\tilde{z}_2^* \sum_{m=1}^N \frac{\tilde{a}_m^*}{2^{m-1}} \binom{m}{\frac{m+1}{2}} [\tilde{z}_2 \tilde{z}_2^*]^{(m-1)/2} \right] \right\} \\ &= E \left[\tilde{z}_1 \tilde{z}_2^* \sum_{n=1}^N \sum_{m=1}^N \frac{\tilde{a}_n \tilde{a}_m^*}{2^{n+m-1}} \binom{n}{\frac{n+1}{2}} \binom{m}{\frac{m+1}{2}} \right. \\ &\quad \cdot \left. \left(\frac{m+1}{2} \right) [\tilde{z}_1 \tilde{z}_1^*]^{(n-1)/2} [\tilde{z}_2 \tilde{z}_2^*]^{(m-1)/2} \right] \\ &= \sum_{n=1}^N \sum_{m=1}^N \frac{\tilde{a}_n \tilde{a}_m^*}{2^{n+m-1}} \binom{n}{\frac{n+1}{2}} \binom{m}{\frac{m+1}{2}} \\ &\quad \cdot E \left[\tilde{z}_1 \tilde{z}_2^* (\tilde{z}_1 \tilde{z}_1^*)^{(n-1)/2} (\tilde{z}_2 \tilde{z}_2^*)^{(m-1)/2} \right]. \end{aligned} \quad (\text{A.7})$$

The computation of (A.7) requires finding a closed-form expression for the expected value

$$E \left[\tilde{z}_1^{(n+1)/2} (\tilde{z}_1^*)^{(n-1)/2} \tilde{z}_2^{(m-1)/2} \tilde{z}_2^* (\tilde{z}_2^*)^{(m+1)/2} \right]. \quad (\text{A.8})$$

To induce a general expression for this expectation, consider the following expansions of (A.8):

$$\begin{aligned} n=1, m=3: \\ E \left[\tilde{z}_1 \tilde{z}_2 (\tilde{z}_2^*)^2 \right] &= 2 \tilde{R}_{zz}(\tau) R_{z_o} \\ n=3, m=3: \\ E \left[\tilde{z}_1^2 \tilde{z}_2 \tilde{z}_1^* (\tilde{z}_2^*)^2 \right] &= 4 \tilde{R}_{zz}(\tau) R_{z_o}^2 + 2 \tilde{R}_{zz}^2(\tau) \tilde{R}_{zz}^*(\tau) \\ n=1, m=5: \\ E \left[\tilde{z}_1 \tilde{z}_2^2 (\tilde{z}_2^*)^3 \right] &= 6 \tilde{R}_{zz}(\tau) R_{z_o}^2 \\ n=3, m=5: \\ E \left[\tilde{z}_1^2 \tilde{z}_2 \tilde{z}_1^* (\tilde{z}_2^*)^3 \right] &= 12 \tilde{R}_{zz}(\tau) R_{z_o}^3 + 12 \tilde{R}_{zz}^2(\tau) \tilde{R}_{zz}^*(\tau) R_{z_o} \\ n=5, m=5: \\ E \left[\tilde{z}_1^3 \tilde{z}_2^2 (\tilde{z}_1^*)^2 (\tilde{z}_2^*)^3 \right] &= 36 \tilde{R}_{zz}(\tau) R_{z_o}^4 + 72 \tilde{R}_{zz}^2(\tau) \tilde{R}_{zz}^*(\tau) R_{z_o}^2 \\ &\quad + 12 \tilde{R}_{zz}^3(\tau) \left[\tilde{R}_{zz}^*(\tau) \right]^2 \\ n=1, m=7: \\ E \left[\tilde{z}_1 \tilde{z}_2^3 (\tilde{z}_2^*)^4 \right] &= 24 \tilde{R}_{zz}(\tau) R_{z_o}^3 \\ n=3, m=7: \\ E \left[\tilde{z}_1^2 \tilde{z}_1^* \tilde{z}_2^3 (\tilde{z}_2^*)^4 \right] &= 48 \tilde{R}_{zz}(\tau) R_{z_o}^4 + 72 \tilde{R}_{zz}^2(\tau) \tilde{R}_{zz}^*(\tau) R_{z_o}^2 \\ n=5, m=7: \\ E \left[\tilde{z}_1^3 \tilde{z}_2^3 (\tilde{z}_1^*)^2 (\tilde{z}_2^*)^4 \right] &= 144 \tilde{R}_{zz}(\tau) R_{z_o}^5 + 432 \tilde{R}_{zz}^2(\tau) \tilde{R}_{zz}^*(\tau) R_{z_o}^3 \\ &\quad + 144 \tilde{R}_{zz}^3(\tau) \left[\tilde{R}_{zz}^*(\tau) \right]^2 R_{z_o} \end{aligned}$$

$n = 7, m = 7:$

$$\begin{aligned} E & \left[\tilde{z}_1^3 \tilde{z}_2^3 (\tilde{z}_1^*)^3 (\tilde{z}_2^*)^4 \right] \\ & = 576 \tilde{R}_{zz}(\tau) R_{zo}^6 + 2592 \tilde{R}_{zz}^2(\tau) \tilde{R}_{zz}^*(\tau) R_{zo}^4 \\ & \quad + 1728 \tilde{R}_{zz}^3(\tau) \left[\tilde{R}_{zz}^*(\tau) \right]^2 R_{zo}^2 \\ & \quad + 144 \tilde{R}_{zz}^4(\tau) \left[\tilde{R}_{zz}^*(\tau) \right]^3 \end{aligned}$$

where $R_{zo} = R_{zz}(0)$.

Collecting terms of equal order yields the following.

Linear Term:

$$\tilde{R}_{zz}(\tau) \left| \tilde{a}_1 + 2\tilde{a}_3 R_{zo} + 6\tilde{a}_5 R_{zo}^2 + 24\tilde{a}_7 R_{zo}^3 + 120\tilde{a}_9 R_{zo}^4 \right|^2.$$

Third-Order Term:

$$1!2! \tilde{R}_{zz}^2(\tau) \tilde{R}_{zz}^*(\tau) \left| \tilde{a}_3 + 6\tilde{a}_5 R_{zo} + 36\tilde{a}_7 R_{zo}^2 + 240\tilde{a}_9 R_{zo}^3 \right|^2.$$

Fifth-Order Term:

$$2!3! \tilde{R}_{zz}^3(\tau) \left[\tilde{R}_{zz}^*(\tau) \right]^2 \left| \tilde{a}_5 + 12\tilde{a}_7 R_{zo} + 120\tilde{a}_9 R_{zo}^2 \right|^2.$$

Seventh-Order Term:

$$3!4! \tilde{R}_{zz}^4(\tau) \left[\tilde{R}_{zz}^*(\tau) \right]^3 \left| \tilde{a}_7 + 15\tilde{a}_9 R_{zo} \right|^2.$$

Ninth-Order Term:

$$4!5! \tilde{R}_{zz}^5(\tau) \left[\tilde{R}_{zz}^*(\tau) \right]^4 \left| \tilde{a}_9 \right|^2.$$

Combining these results, a closed-form expression can be derived for the gain compression term

$$\begin{aligned} \tilde{R}_{zz}(\tau) & \sum_{n=1}^N \sum_{m=1}^N \frac{n!m!}{2^{n+m-2}} \binom{n+1}{2} \binom{m+1}{2} R_{zo}^{(n+m-2)/2} \tilde{a}_n \tilde{a}_m^* \\ & = \tilde{R}_{zz}(\tau) \left[1! \tilde{a}_1 + 2! \frac{3}{4} \tilde{a}_3 R_{zo} + 3! \frac{5}{8} \tilde{a}_5 R_{zo}^2 + 4! \frac{35}{64} \tilde{a}_7 R_{zo}^3 \right. \\ & \quad \left. + \cdots + \frac{N!}{2^{N-1}} \binom{N+1}{2} \tilde{a}_N R_{zo}^{(N-1)/2} \right] \\ & \quad \times \left[1! \tilde{a}_1^* + 2! \frac{3}{4} \tilde{a}_3^* R_{zo} + 3! \frac{5}{8} \tilde{a}_5^* R_{zo}^2 + 4! \frac{35}{64} \tilde{a}_7^* R_{zo}^3 \right. \\ & \quad \left. + \cdots + \frac{N!}{2^{N-1}} \binom{N+1}{2} \tilde{a}_N^* R_{zo}^{(N-1)/2} \right] \\ & = \tilde{R}_{zz}(\tau) A A^* \end{aligned} \quad (A.9)$$

where

$$A = \left[\sum_{n=1}^N \frac{n!}{2^{n-1}} \binom{n+1}{2} \tilde{a}_n R_{zo}^{(N-1)/2} \right].$$

A closed-form expression can be induced from successive expansions of (A.8), yielding the general-output autocorrelation function of the nonlinear device as a function of the statistics of the input stream, $R_{zz}(\tau)$. This, however, requires overwhelmingly complex manual expansion of the moment expressions. This procedure also generates crossterms $[R_{zo}$

terms, as opposed to (14), which depends only on $R_{zz}(\tau)$] that are expected to account for compression effects.

REFERENCES

- [1] J. F. Sevic, M. B. Steer, and A. M. Pavio, "Nonlinear analysis methods for the simulation of digital wireless communication systems," *Int. J. Microwave Millimeter-wave Computer Aided Eng.*, vol. 6, no. 3, pp. 197–216, 1996.
- [2] J. F. Sevic and M. B. Steer, "Analysis of GaAs MESFET spectrum regeneration driven by a DQPSK modulated source," in *IEEE MTT-S Int. Microwave Symp. Dig.*, June 1995, pp. 1375–1378.
- [3] N. Borges and J. C. Pedro, "Simulation of multitone IMD distortion and spectral regrowth using spectral balance," in *IEEE MTT-S Int. Microwave Symp. Dig.*, June 1998, pp. 729–732.
- [4] J. F. Sevic, M. B. Steer, and A. M. Pavio, "Large signal automated load-pull of adjacent channel power for digital wireless communication systems," in *IEEE MTT-S Int. Microwave Symp. Dig.*, June 1996, pp. 763–766.
- [5] A. Leke and J. S. Kenney, "Behavioral modeling of narrow-band microwave power amplifiers with applications in simulating spectral regrowth," in *IEEE MTT-S Int. Microwave Symp. Dig.*, June 1996, pp. 1385–1388.
- [6] S. W. Chen, W. Pantou, and R. Gilmore, "Effects of nonlinear distortion on CDMA communication systems," *IEEE Trans. Microwave Theory Tech.*, vol. 44, pp. 2743–2749, Dec. 1996.
- [7] J. Lajoinie, E. Ngoya, D. Barataud, J. Nebus, J. Sombrin, and B. Riviere, "Efficient simulation of NPR for the optimum design of satellite transponders SSPA's," in *IEEE MTT-S Int. Microwave Symp. Dig.*, June 1998, pp. 741–744.
- [8] J. F. Sevic and J. Staudinger, "Simulation of power amplifier adjacent channel power ratio for digital wireless communication systems," in *IEEE MTT-S Int. Microwave Symp. Dig.*, June 1997, pp. 681–685.
- [9] R. F. Baum, "The correlation function of smoothly limited Gaussian noise," *IRE Trans. Inform. Theory*, vol. IT-3, pp. 193–196, Sept. 1957.
- [10] O. Shimbo, "Effects of intermodulation, AM-PM conversion and additive noise in multicarrier TWT systems," *Proc. IEEE*, vol. 59, pp. 230–238, Feb. 1971.
- [11] E. Bedrosian and S. O. Rice, "The output properties of Volterra systems (Nonlinear systems with memory) driven by harmonic and Gaussian inputs," *Proc. IEEE*, vol. 59, pp. 1688–1707, Dec. 1971.
- [12] Q. Wu, M. Testa, and R. Larkin, "On design of linear RF power amplifiers for CDMA signals," *Int. J. Microwave Millimeter-wave Computer Aided Eng.*, vol. 8, no. 3, pp. 283–292, 1998.
- [13] Q. Wu, H. Xiao, and F. Li, "Linear RF power amplifier design for CDMA signals: A spectrum analysis approach," *Microwave J.*, pp. 22–40, Dec. 1998.
- [14] M. C. Jeruchim, P. Balaban, and K. S. Shanmugan, *Simulation of Communication Systems*. New York: Plenum, 1992.
- [15] J. Staudinger, "Applying quadrature modeling technique to wireless power amplifiers," *Microwave J.*, vol. 40, no. 11, pp. 66–86, Nov. 1997.
- [16] G. L. Heiter, "Characterization of nonlinearities in microwave devices and systems," *IEEE Trans. Microwave Theory Tech.*, vol. MTT-21, pp. 797–805, Dec. 1973.
- [17] *Mobile Station-Base Station Compatibility Standard for Dual-Mode Wideband Spread-Spectrum Cellular Systems*, TIA/EIA Standard IS-95, 1993.
- [18] H. Gutierrez, K. Gard, and M. B. Steer, "Spectral regrowth in nonlinear amplifiers using transformation of signal statistics," presented at the 1999 IEEE MTT-S Int. Microwave Symp.
- [19] J. G. Proakis, *Principles of Digital Communications*. New York: McGraw-Hill, 1995.
- [20] M. B. Steer and P. J. Khan, "An algebraic formula for the output of a system with large-signal, multifrequency excitation," *Proc. IEEE*, vol. 71, pp. 177–179, Jan. 1983.
- [21] M. B. Steer, C. R. Chang, and G. W. Rhyne, "Computer-aided analysis of nonlinear microwave circuits using frequency domain nonlinear analysis techniques: The state of the art," *Int. J. Microwave Millimeter-wave Computer Aided Eng.*, vol. 1, no. 2, pp. 181–200, 1991.
- [22] I. S. Reed, "On a moment theorem for complex Gaussian processes," *IEEE Trans. Inform. Theory*, vol. IT-8, pp. 194–195, Apr. 1962.
- [23] V. Aparin, K. Gard, G. Klemens, and C. Persico, "GaAs RFIC's for CDMA/AMPS dual-band wireless transmitters," in *IEEE MTT-S Int. Microwave Symp. Dig.*, June 1998, pp. 81–84.
- [24] J. G. Proakis and D. G. Manolakis, *Digital Signal Processing: Principles, Algorithms, and Applications*, 2nd ed. New York: Macmillan, 1992, ch. 12.

- [25] W. Zhang and M. J. Miller, "Baseband equivalents in digital communication system simulation," *IEEE Trans. Education.*, vol. 35, pp. 376–382, Apr. 1992.



Kevin G. Gard (S'92–M'95) was born in Raleigh, NC, in 1966. He received the B.S. (with honors) and M.S. degrees in electrical engineering from North Carolina State University, Raleigh, in 1994 and 1995, respectively, and is currently working toward the Ph.D. degree in electrical engineering at the University of California at San Diego.

Since 1996, he has been with Qualcomm Inc., San Diego, CA, where he is a Senior Engineer responsible for the design and development of radio-frequency integrated circuits (RFIC's) for code-division multiple-access (CDMA) wireless products. He has designed GaAs metal–semiconductor field-effect transistor (MESFET) and Si BiCMOS integrated circuits for cellular and personal communication systems (PCS) CDMA transmitter applications. His research interests are in the areas of integrated circuit design for wireless applications and analysis of nonlinear microwave circuits with digitally modulated signals.

Mr. Gard is a member of the IEEE Microwave Theory and Techniques and Solid-State Circuits Societies, Eta Kappa Nu, and Tau Beta Pi.



Hector M. Gutierrez (S'97–M'98) received the B.Sc. degree in applied mathematics from the Universidad Cayetano Heredia, Lima, Peru, in 1989, the B.Sc. degree in mechanical engineering from the Pontificia Universidad Catolica, Lima, Peru, in 1991, and the M.Eng. degree in manufacturing systems engineering and the Ph.D. degree in electrical engineering from North Carolina State University, Raleigh, in 1992 and 1997, respectively.

After working for two years as Lecturer in the Department of Mathematics and Physics, Universidad Cayetano Heredia, he joined North Carolina State University. His professional interests revolve around the various aspects of system modeling, computer interfacing and automatic control of electromechanical systems. From 1997 to 1999, he was with the Center for Advanced Computing and Communication, North Carolina State University, where he developed behavioral models of nonlinear microwave amplifiers and simulation tools for modeling electro-thermal circuit interactions. He is currently with the Mechanical Engineering Program, Division of Engineering Sciences, Florida Institute of Technology, Melbourne, FL.



Michael B. Steer (S'76–M'78–SM'90–F'99) received the B.E. and Ph.D. degrees in electrical engineering from the University of Queensland, Brisbane, Australia, in 1978 and 1983 respectively.

From 1983 to 1999, he was with the Department of Electrical and Computer Engineering, North Carolina State University, Raleigh, as a Professor. His expertise in teaching and research involved circuit- design methodology. In 1999, he joined the School of Electronic and Electrical Engineering, The University of Leeds, Leeds, U.K., as Chair of

Microwave and Millimeter-Wave Electronics and Director of the Institute of Microwaves and Photonics. From a teaching perspective, he has taught courses at the sophomore through advanced graduate level in circuit design, including basic circuit design, analog integrated-circuit design, RF and microwave circuit design, solid-state devices, and computer-aided circuit analysis. He teaches video-based courses on computer-aided circuit analysis and on RF and microwave circuit design, which are broadcast nationally by the National Technological University. His research has been directed at developing RF and microwave design methodologies, tied to the development of microwave circuits and solving fundamental problems, in both high-speed digital and microwave circuit implementations. Until 1996, he was the Librarian of the industry-based IBIS consortium, which provides a forum for developing behavioral models. A converter written by his group to automatically develop behavioral models from a SPICE netlist is being used by upwards of 100 companies and has been incorporated in several commercial computer-aided engineering programs. He had developed area-efficient microwave measurement techniques, which are being used in the electrical characterization of high-performance integrated circuits and multichip modules. Currently, his interest in RF and microwave design are the computer-aided global modeling of large microwave and millimeter-wave system spatial power-combining systems, the implementation of a two-dimensional quasi-optical power-combining system, and high-efficiency and low-cost RF technologies for wireless applications. He has organized many workshops and taught many short courses on signal integrity, wireless, and RF design. He has authored or co-authored over 150 papers and book chapters on topic related to RF and microwave design methodology.

Dr. Steer is a member of the International Union of Radio Science (URSI), Commission D. He is active in the IEEE Microwave Theory and Techniques Society (MTT-S). In 1997, he was secretary of the IEEE MTT-S and is an elected member of the Administrative Committee for the 1998–2001 term. In the IEEE MTT-S, he also serves on the technical committees on field theory and on computer-aided design. He is a 1987 Presidential Young Investigator and, in 1994 and 1996, was awarded the Bronze Medallion for Outstanding Scientific Achievement presented by the Army Research Office.